Surface studies of spin-polarized atomic hydrogen

L. Pollack,* S. Buchman,† and T. J. Greytak
Department of Physics and Center for Materials Science and Engineering, Massachusetts Institute of Technology, Cambridge, Massachusetts 02139
(Received 9 July 1991)

We present the results of a series of experiments on spin-polarized atomic hydrogen in an environment with a large amount of surface area. Both nuclear-magnetic-resonance and pressure-transducer techniques were used. The NMR measurements yield a value for the hyperfine wall shift of $-22.4(5)$ kHz at 7.62 T. The results were consistent with a sticking probability of $[0.33(2)]T$ for atomic hydrogen on a superfluid ^{4}He surface for atom temperatures near 0.15 K. Using the pressure transducer, we have measured the decay of the polarized gas due to dipole-dipole interactions between adsorbed hydrogen atoms. At 7.62 T, with the surface normal at right angles to the applied field, we measure $G_s=[2.5(3)]\times10^{-14}$ cm^2/sec. We have also observed a small increase in G_s as a function of decreasing magnetic field.

I. INTRODUCTION

The surfaces of any cell used to confine spin-polarized atomic hydrogen are critical to the stability of the gas. At modest densities only a small amount of recombination occurs in the bulk. The majority of the recombination events take place on the surface. Moreover, the byproducts of that reaction—molecular hydrogen and the recombination energy—are ultimately deposited there. Electron and nuclear spin relaxation processes, which also destabilize the gas, take place on the surface. The surface covering of choice is liquid helium. Of all materials, it has the smallest van der Waals attraction to hydrogen, and therefore results in the lowest possible surface density of hydrogen atoms for a given bulk density. The interaction is so weak that even at the lowest temperatures no more than a single monolayer of atomic hydrogen can be adsorbed onto the surface.

The adsorbed monolayer of atomic hydrogen is interesting in its own right as a novel two-dimensional quantum fluid. At low densities the atoms undergo diffusion[1] in two dimensions as they are scattered by ripplons, the quantized surface excitations of the helium film. At intermediate densities the atomic hydrogen gas should support two-dimensional nuclear spin waves,[2] similar to those already observed in the bulk gas.[3] At a high enough surface density and low enough temperature, the adsorbed atoms should undergo a Kosterlitz-Thouless[4] transition to a superfluid state.

We present measurements of three quantities that probe different aspects of the interaction between spin-polarized atomic hydrogen and a film of superfluid ^{4}He: the wall shift,[5] the sticking probability,[6–10] and the nuclear spin relaxation rate.[11] The first two quantities are determined from nuclear-magnetic-resonance measurements of atoms on the surface and in the bulk, the third is found by monitoring the decay rate of the atomic density. The wall shift is a measure of the change in the hyperfine interaction between the electron and the proton which results when a hydrogen atom is adsorbed onto the surface. We find a wall shift of $\delta=-22.4(5)$ kHz for the hyperfine frequency in a magnetic field of 7.62 T. This corresponds to a shift of $\delta=-43.2(10)$ kHz in the zero-field hyperfine resonance frequency. The sticking probability is the probability that an atom will become adsorbed during a collision with the surface. If we assume that $s\propto T$, we find that our results are best fit by the expression $s=0.33(2)T$ for temperatures in the vicinity of 0.11–0.24 K. This is in agreement with previous values obtained by different techniques.[8–10] Nuclear spin relaxation results from the fluctuating magnetic field experienced at the nucleus of an atom due to the electronic moments of other atoms passing by in the gas. We find a relaxation rate constant $G_s=[2.5(3)]\times10^{-14}$ cm^2/sec for surfaces oriented parallel to the applied magnetic field.

II. BACKGROUND

A. Adsorption

Consider a cell containing a gas of hydrogen atoms of uniform density n in thermal equilibrium with the walls at a temperature T. A surface density σ of hydrogen atoms will be adsorbed on the surface of the superfluid helium film coating the walls of the cell. For high temperatures and low bulk densities the relation between σ, n, and T is given by the classical adsorption isotherm

$$\sigma=n\Lambda\exp\left[\frac{E_b}{kT}\right], \tag{1}$$

where $\Lambda=h/\sqrt{2\pi mkT}$ is the thermal de Broglie wavelength and E_b is the binding energy of the atom to the surface. For atomic hydrogen, Λ in Å is $17.4/\sqrt{T}$ and E_b is 1.04 K on a saturated ^{4}He film.[12] If the temperature is lowered while keeping the bulk density constant, the surface density will first rise slightly above the value given by Eq. (1) due to statistical effects associated with the Bose character of the hydrogen atoms. As the temperature drops further, the surface density will finally saturate at a finite value due to the interactions between the

hydrogen atoms on the surface. The complete isotherms are displayed in Fig. 1 which is adapted from Ref. 13. The experimental measurements reported here were carried out in the region where the "classical" relationship applies.

An important parameter for determining the dynamics of spin-polarized hydrogen is the ratio of the number of atoms on the surface, N_s, to the number in the bulk, N_b. This depends only on the area to volume ratio, A/V, and the adsorption isotherm. By the principal of detailed balance, this ratio is also equal to the ratio of the mean time that an atom spends on the surface, τ_s, and the mean time it spends in the bulk between adsorption events, τ_b:

$$\frac{N_s}{N_b}=\frac{\tau_s}{\tau_b}=\frac{A}{V}\frac{\sigma}{n}\approx\frac{A}{V}\Lambda(T)\exp\left[\frac{E_b}{kT}\right] . \tag{2}$$

The flux of atoms striking a unit area of wall from the gas is given by $\phi=nv/4$, where $v=\sqrt{8kT/\pi M}$ is the mean speed of the gas atoms. By equating the rate at which atoms leave the surface to that which they collide and stick, one can determine the mean residence time on the surface:

$$\tau_s=\frac{\sigma}{\phi s}=\frac{\Lambda}{s}\left[\frac{2\pi M}{kT}\right]^{1/2}\exp\left[\frac{E_b}{kT}\right] . \tag{3}$$

As expected, τ_s depends only on the intrinsic properties of the surface and the sticking probability, s. Equation (3) assumes that the sticking coefficient is a simple constant. For the more physical situation where s depends on the energy and incident angle of the incoming atom, Eq. (3) will have to be modified by using a suitably averaged value for s.

B. Hyperfine states

The ground ($1S$) state of atomic hydrogen is split into four nondegenerate hyperfine levels in the presence of an external magnetic field as shown in Fig. 2. These states are referred to as the $|a\rangle$, $|b\rangle$, $|c\rangle$, and $|d\rangle$ state in order of increasing energy. In terms of the basis of electron and proton spin projection, $|m_s, m_i\rangle$, the states can be written as follows:

$$|a\rangle=\cos\theta|-\tfrac{1}{2},\tfrac{1}{2}\rangle-\sin\theta|\tfrac{1}{2},-\tfrac{1}{2}\rangle ,$$

$$|b\rangle=|-\tfrac{1}{2},-\tfrac{1}{2}\rangle ,$$

$$|c\rangle=\cos\theta|\tfrac{1}{2},-\tfrac{1}{2}\rangle+\sin\theta|-\tfrac{1}{2},\tfrac{1}{2}\rangle ,$$

$$|d\rangle=|\tfrac{1}{2},\tfrac{1}{2}\rangle .$$

The hyperfine mixing angle θ is defined as

$$\tan(2\theta)=\frac{A_0}{h(\gamma_e+\gamma_p)B}=0.050\,61/B . \tag{4}$$

In this expression A_0 is the hyperfine constant for the ground state of atomic hydrogen, 1420 MHz, γ_e and γ_p are the electron and proton gyromagnetic ratios, and B is the magnetic field in T. At temperatures that are small compared to the $|b\rangle$-$|c\rangle$ splitting, approximately 10 K in a field of 7.62 T, the gas that initially fills the cell is composed of roughly equal numbers of $|a\rangle$ and $|b\rangle$ states. For this field the mixing angle is so small, $\theta\approx10^{-3}$, that the gas is predominantly electron spin polarized. Yet the fact that θ is not exactly zero allows for a slow recombination into molecular hydrogen. In a fraction of the collisions the electron spins of the two hydrogen atoms will be antiparallel. In high fields this fraction is θ^2 for $|a\rangle$-$|b\rangle$ collisions and $2\theta^2$ for $|a\rangle$-$|a\rangle$ collisions. Recombination into molecules will occur in these cases only if a third body is present to satisfy momentum and energy conservation. The third body can only be another hydrogen atom or the occasional helium atom when the collision occurs in the bulk gas.[14] When the atoms are adsorbed on the surface, the surface itself plays the role of the third body. Collisions between two $|b\rangle$ atoms will not result in recombination because the electron spins of the two atoms are always parallel. As a result of this state-dependent recombination, the electron polarized gas evolves to a doubly polarized gas containing predominantly $|b\rangle$ atoms.[11,14]

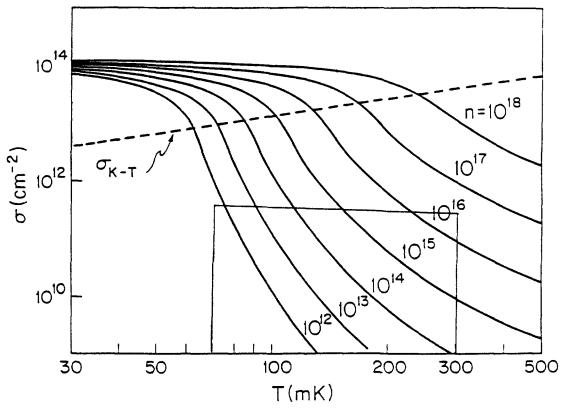

FIG. 1. Surface density as a function of temperature taking interatomic forces into account. Each curve represents the equilibrium surface density for the specified bulk density. The dashed line shows the density required to reach the Kosterlitz-Thouless transition. The enclosed region shows the regime of interest to these experiments where the simpler ideal-gas law expression, Eq. (1), is valid.

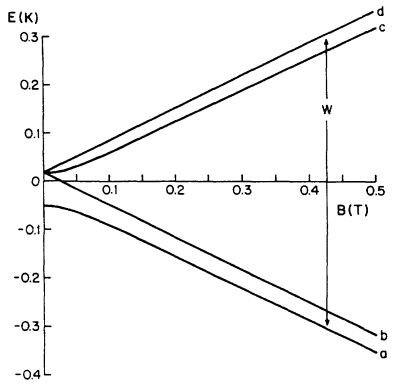

FIG. 2. The hyperfine diagram of the $1S$ state of atomic hydrogen. The spacing between the $|a\rangle$ state and the $|d\rangle$ state is about 10 K at $B=8$ T.

C. Relaxation

The gas of $|b\rangle$ atoms is stable only on a time scale on the order of the longitudinal relaxation time (Ref. 8) since the atoms eventually relax to the $|a\rangle$ state which has a lower energy. The mechanism for this relaxation is the dipole-dipole interaction between two colliding hydrogen atoms. Once a $|b\rangle$ atom relaxes into the $|a\rangle$ state, recombination with a $|b\rangle$ atom occurs very rapidly. Under these circumstances the rate of decay of the density is determined by the slower process: it is governed by the relaxation rather than the recombination rate coefficient. The degree of nuclear polarization of the gas, however, is determined by the ratio of the two rate coefficients.[13]

The two-body relaxation can occur in the bulk or on the surface. Both processes contribute to an effective two-body relaxation rate in which the relaxation on the surface is expressed in terms of its effect on the bulk density:[13]

$$G_{\text{eff}}=G_b+G_s\frac{A}{V}\left[\Lambda\exp\left[\frac{E_b}{kT}\right]\right]^2 . \tag{5}$$

G_b has been measured by several groups,[13,15], however G_s is more difficult to measure because its effect is small compared to other dissipative mechanisms on the surface. Several calculations of the magnitude of G_s exist.[16,17] The most detailed calculation[17] yields

$$G_s(\Phi)=1.56[G_{s,0}\sin^2(2\Phi)+G_{s,2}\sin^2(\Phi)(1+\cos^2\Phi)] , \tag{6}$$

where

$$G_{s,0}=(0.96-0.82T+0.74T^2)\times\left[1+\frac{16.683}{B}\right]^2\times10^{-14}\ \text{cm}^2\,\text{sec}^{-1} \tag{7}$$

and

$$G_{s,2}=(0.038+0.278T)\times\left[1+\frac{16.683}{B}\right]^2\times10^{-14}\ \text{cm}^2\,\text{sec}^{-1} . \tag{8}$$

This rate is a strong function of the angle Φ between the surface normal and the direction of the magnetic field. It is a maximum near 45° and vanishes for surfaces oriented at 90° to the external field.

When analyzing the decay of the spin-polarized atomic hydrogen there are two other processes which must be considered: three-body recombination and one-body relaxation. The three-body process has both bulk and surface contributions. In addition, it permits the recombination of three $|b\rangle$ state atoms. Three-body recombination dominates at high densities. These densities occur in the bulk and, when the temperature is low enough, on the surface as well. A more detailed discussion of the three-body rate is beyond the scope of this paper, but can be found in Refs. 12 and 15.

The one-body rate involves the relaxation of a $|b\rangle$ state atom into the $|a\rangle$ state due to an interaction with a magnetic impurity. By assumption this impurity is on the surface, so there is no bulk contribution to this process. A calculation[18] has been done which assumes that the relaxation is due to local magnetic fields caused by magnetic impurities buried under the surface of the liquid-He film. In its motion past an impurity, a hydrogen atom may feel a fluctuating field at the Larmor frequency which can lead to a transition. The relaxation rate under these circumstances is a strong function of the distance between the impurity and the hydrogen atom. Although this calculation is consistent with some experimental results, it seems that the origin of this process is not completely understood.

D. NMR

We have chosen to study the surface processes in two different ways: nuclear-magnetic-resonance (NMR) and density decay measurements. NMR can be used to measure the difference in the $|a\rangle$ and $|b\rangle$ state populations since the states differ predominantly in the direction of nuclear spin projection. The atoms are given a rf pulse at the $|a\rangle$-$|b\rangle$ transition frequency defined by

$$\omega_{ab}=\frac{2\pi A_0}{2}+\gamma_p B+\frac{(2\pi A_0)^2}{4(\gamma_e+\gamma_p)B} , \tag{9}$$

and both the frequency of the transition and the decay time are measured. The constants in this expression are the same as those in Eq. (4). This expression is valid in the high-field limit: $(\gamma_p+\gamma_e)B \gg A_0$. The last term can be ignored with respect to the second. The temperature dependence of the NMR signal yields information about both the wall shift and the sticking probability. At high temperatures ($\sigma A/nV$ very small) the mean time in the bulk τ_b is greater than the mean time on the surface τ_s thus, the measured transition frequency corresponds to that of free atoms. As the temperature is lowered, τ_s increases as atoms become bound to the surface for longer times. The mechanism which is responsible for binding is the van der Waals force between H and He atoms. The distortion of the electron cloud of the hydrogen atom which results from the binding reduces the hyperfine interaction between the electron and proton of a H atom. The resulting change in the zero-field hyperfine frequency, $\delta\equiv A_{\text{wall}}-A_0$, is referred to as the wall shift. The wall shift in nonzero field is expected to reflect the anisotropy of the hyperfine interaction.[19] From the NMR measurements made as a function of temperature, information about both the wall shift and the sticking coefficient can be extracted.[5,20,21]

E. Decay of the density

The second technique measures the sum of the $|a\rangle$ and $|b\rangle$ state densities by monitoring the pressure of the gas (and from the ideal-gas law its density). Once a recombination event occurs, the molecule that is created will quickly freeze out on a surface. By monitoring the decay rate of the atomic density it is possible to determine the mechanisms that are responsible for the recombination. A great deal of experimental and theoretical work has

been devoted to measuring the various relaxation and recombination rates.[22] The rates are distinguished by the number of hydrogen atoms involved as well as the location of the collision (in the bulk or on the surface). As expected, the bulk processes dominate at high temperatures ($nV \gg \sigma A$) and the surface processes dominate at low temperatures ($nV \ll \sigma A$).

For a gas with complete nuclear polarization, in which only the $|b\rangle$ state is present, the time rate of change of density can be written as

$$-\dot{n} = L_{\text{eff}} n^3 + G_{\text{eff}} n^2 + R_{\text{eff}} n \ , \tag{10}$$

where the effective rates contain contributions from both surface and bulk processes. We have used Eq. (10) to obtain values for G_s and estimates of R.

III. EXPERIMENT

Two separate but similar experiments have been carried out to measure the wall shift, sticking probability, and the two-body surface relaxation rate, G_s. We will give detailed descriptions of both experimental cells in this section. In the next section results from both sets of experiments will be described.

Atomic hydrogen is produced by an rf discharge in molecular hydrogen at liquid-nitrogen temperature (see Ref. 12). The atoms are cryopumped into a tube which runs through the center of the dilution refrigerator. The magnetic field produced by an 8-T superconducting solenoid presents a potential well to the atoms of the lower two hyperfine states and a potential barrier to those of the upper two states.

A pressure transducer is mounted on the fill line, below the mixing chamber. It operates by measuring changes in spacing (capacitance) between a thin layer of gold evaporated on a flexible Kapton membrane and a fixed plate. It has a sensitivity of 5×10^{13} atoms/cm^3 Hz and can detect 10^{12} atoms. The pressure transducer is close enough to the cell so that the difference in density due to variations in the field of the magnet is negligible. A schematic of the apparatus below the level of the mixing chamber showing the location of the pressure transducer and the cell is shown in Fig. 3.

Once a saturated film of superfluid ^{4}He is in place and the discharge is lit, atomic hydrogen is produced. The hydrogen is transported through the refrigerator in the same way as described in Ref. 12. The temperature of the fill line can be adjusted with heaters to obtain the maximum fill rate. Hydrogen flow into the cell is measured by a decrease in the cooling power of the refrigerator due to the recombination heating, and by a signal on the pressure transducer. Fluxes as high as 5×10^{14} atoms/sec have been obtained. The discharge must be throttled down for temperatures below 300 mK as the heat load from the recombination exceeds the cooling power of the refrigerator in this regime.

Just below the pressure transducer there is a loop-gap resonator that is enclosed in a 6.3-cm-diam cylindrical can. Figure 4 is a detailed drawing of the resonator. The loop-gap combination (LC) can be tuned by changing either the spacing between the plates by tightening the

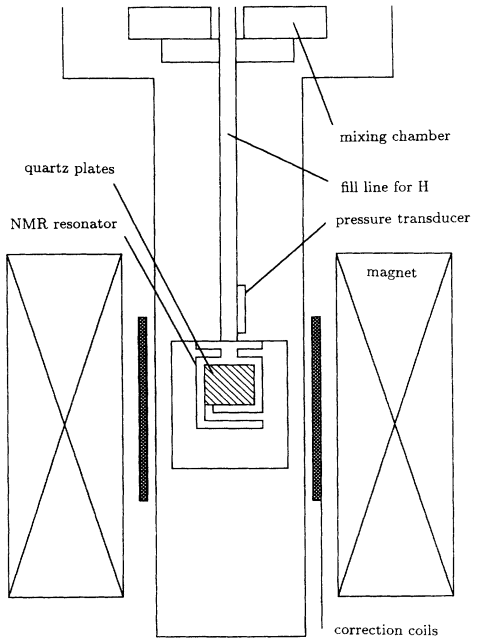

FIG. 3. A schematic of the apparatus is shown below the level of the mixing chamber of the dilution refrigerator.

screws that hold it in place against an indium spacer, or by removing material from one of the capacitor plates. The resonator is tuned at room temperature with allowances made for changes which occur as it is cooled. The resonant frequency of the cavity is approximately 1 GHz, which corresponds to the $|a\rangle$-$|b\rangle$ splitting when a field of 7 T is applied.

The substrate for the studies is contained in the loop (inductive) part of the resonator and consists of 55 1.6-cm square crystalline quartz plates of thickness 150 μm separated along the edges by 75-μm Kapton spacers. The plates are oriented so that the surfaces lie parallel to the direction of the applied field. Crystalline quartz was chosen because of its high thermal conductivity. The surface roughness of the plates, as determined by an electron

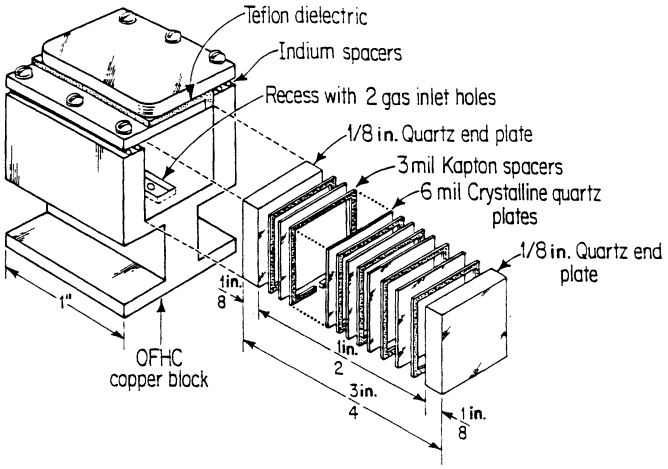

FIG. 4. This figure shows a more complete drawing of the NMR resonator.

microscope picture, is on the order of 1 μm, which is less than the capillary radius of a saturated film of superfluid ^{4}He. The He-covered plates therefore present a smooth surface to the H atoms. Under typical experimental heat loads, the temperature difference between the ^{4}He film and the quartz plates due to the Kapitza boundary resistance is less than 1 mK. The spacers that separate the plates have a small opening along one edge to allow the hydrogen gas to enter the interplate region. On each end there are two 3-mm-thick plates which provide mechanical stability. The area to volume ratio of this substrate is equal to $2/d$, where d is the spacing between the plates. In this case, $A/V=263$ cm^{-1}. The total surface area of the quartz plates that is accessible to the hydrogen is 178 cm^2. The edges of this package were sealed with Stycast 1266 epoxy to confine the atoms to a region of known A/V ratio and to provide increased thermal contact between the plates and the copper resonator.

The hydrogen enters this region through two small holes that are drilled through the top of the resonator. The time that it takes for an atom to travel the length of these holes is greater than the polarization time at 80 mK. At the exit of these holes a channel is milled into the resonator to allow the hydrogen to enter each interplate region. The openings in the spacers are carefully aligned with this channel. The diameter of the two fill holes is beyond the cutoff frequency for the rf used for the NMR so that the atomic signal that we see comes from the atoms in the interplate region only.

A gradient coil assembly is mounted inside the bore of the magnet but outside of the vacuum can. Its center coincides with that of the magnet. There are six independent coils which allow for the application of linear or quadratic corrections to B_z in each spatial direction. Fields of several G result for currents of about 1 A.

Two different thermometers are used for the experimental measurements. A Matsushita 100Ω carbon resistor mounted at the bottom of the NMR can measures the temperature of the copper can and may be used for temperature control of the cell. All of the quoted temperatures have been measured with a carbon thermometer, made by sandwiching a small amount of Aerodag[23] between two thin layers of Ag paint.[24] The thermometer sits inside the resonator on one of the quartz plates. (This thermometer will be referred to as the plate thermometer in the experimental section.) All of the thermometers were calibrated at high field against a ^{3}He melting curve thermometer[25] at the start and end of each run.

The NMR spectrometer used to make the measurements is a two-phase homodyne spectrometer which is optimized for operation at 1 GHz. The spectrometer is operated in transmission mode; separate coupling loops located at the two openings of the inductor are used to aid in isolation of the transmitter from the receiver. All of the electronics operate at room temperature with the exception of a GaAs field-effect-transistor (FET) amplifier on the receiver arm which sits in the 4-K bath. The spectrometer is calibrated by comparing the amplitude of the NMR signal with the density derived from the pressure transducer in a regime where the polarization (defined as the difference in population between the b and a states divided by their sum) is known to be close to unity.

A second version of the cell was designed with the goal of measuring the decay rate of the atomic gas. The design is very similar to the first cell with the following modifications. The size of the Kapton spacers was reduced from 75 to 25 μm, which triples the area to volume ratio. The total surface area is also increased because more plates can be fit inside the resonator. Additionally, a system which allows the preplating of the quartz surfaces with a layer of molecular H_2 at high temperature ($T>20$ K) was constructed to increase the distance between the atom and any magnetic impurity at the quartz surface. This system consists of a thin capillary that runs from a room-temperature gas handling system through the Dewar space, enters the vacuum can, wraps around the NMR can several times, and comes back up through the Dewar to room temperature. During a bakeout, He gas can be pumped through this tube (with the rest of the refrigerator held at 20 K by heaters). This gas is cooled through contact with the liquid He in the Dewar and will preferentially cool the cell. As the cell is being cooled, molecular H_2 can be introduced into the experimental space.[26] The hydrogen will plate out onto the coldest surfaces which are the NMR resonator and the quartz plates. It is not possible to make any direct measurement of the thickness or uniformity of the coating, except in terms of its influence on the one-body rate. In all experiments, saturated ^{4}He films were employed; we tried increasing the amount of ^{4}He present and observed no changes in the measured decay rates. The amount of ^{4}He present in the cell was never enough to allow for the collection of bulk liquid between the plates.

Other changes in the experimental setup include the use of a two-stage GaAs FET amplifier which can detect 2×10^{12} atoms in a 30-kHz bandwidth and a change in the location of the Aerodag thermometer. The thermometer is mounted $\frac{1}{3}$ of the way into the package instead of on an end plate.

IV. RESULTS

Two groups of results are presented. One group, from experiments made on the first cell, involved the NMR properties of the combined surface and bulk system. The other group of results, from the modified cell, comes from a study of the decay.

A. NMR measurements

The NMR spectrum of spin-polarized atomic hydrogen was studied by measuring the response of the atoms to a pulse of rf applied near the Larmor frequency at a variety of temperatures. Results of several days of temperature scans are shown in Fig. 5. Each point is the result of a fit of a given free-induction-decay (FID) signal to an exponentially decaying sinusoid. The quoted temperature at each point is the temperature of the plate (Aerodag) thermometer.

We can understand the qualitative behavior of the system as follows: at high temperatures, when the time in the bulk is much larger than the time on the surface, the atoms resonate at the pure bulk frequency. As the tem-

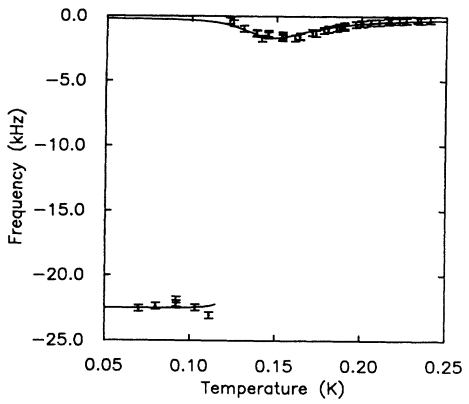

FIG. 5. The frequency of the $|a\rangle$-$|b\rangle$ transition is shown as function of temperature. Each data point is the result of fitting a free-induction-decay signal to a decaying exponential function. The upper, higher-frequency branch represents the signal from the atoms in the bulk; the lower branch corresponds to atoms that are adsorbed on the surface.

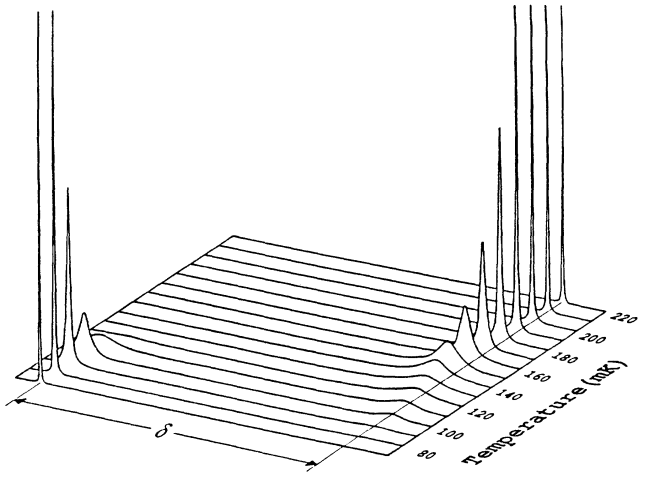

FIG. 6. The predictions of Eq. (11) are displayed as Fourier transform spectra at various temperatures. The frequency of the center of the line corresponds to the value of frequency determined by fitting the free-induction-decay signal.

perature is lowered, so that τ_s increases, the fraction s of atoms that stick to the wall has a smaller resonance frequency for the time that they are adsorbed on the wall since the hyperfine interaction of the adsorbed atoms is weaker. If τ_s is very small with respect to τ_b, the atoms return to the bulk, but they are dephased slightly with respect to atoms that did not experience a sticking event. Thus, as the temperature is decreased, the mean frequency of the line shifts slightly towards the surface frequency and the width increases due to the dephasing. Eventually, as the temperature is lowered so that τ_s is no longer small with respect to τ_b, the adsorbed atoms remain on the surface for much longer times and are completely dephased if they desorb. The only atoms that contribute to the bulk signal are those which have had short sticking events in the observation time, so the frequency shifts back towards its free value. Finally, when the sticking time becomes longer than the observation time, a second line appears at the wall-shifted position. This is the behavior that we observe as shown in Fig. 5. From the measured difference in frequency, we extract a value for the wall shift δ. (In this case, it is the parallel wall shift, since all of the surface area is aligned parallel to the direction of the external field.) We find that $\delta=-22.4(5)$ kHz. It is also clear that the behavior of the system depends critically on the value of τ_s which, if the temperature and area to volume ratio are known, yields an experimental value for the sticking probability.

We fit the data of Fig. 5 to a model developed by Anderson and Weiss[27] which predicts the behavior of an atom in an environment which has two separate resonance frequencies. The parameter that determines the behavior of the resonance line as a function of temperature is the ratio of the transition probability per unit time between the two environments to the difference in frequency between the two environments (wall shift). The transition probability is related to τ_b and τ_s, thus, from Eqs. (2) and (3), it depends on the sticking probability, the area to volume ratio, as well as the wall shift. The results of a calculation of the adsorption line shape are shown in Fig. 6 for reasonable values of each of the parameters. The expression for the line intensity as a function of frequency is

$$I(\omega,T)=\frac{\Gamma a(a-1)(\omega_b-\omega_s)^2}{(\omega-\omega_b)^2(\omega-\omega_s)^2+\Gamma^2[(1-a)(\omega-\omega_b)+a(\omega-\omega_s)]^2}\ . \tag{11}$$

In this expression $\Gamma=1/\tau_s+1/\tau_b$, $a=\tau_s/(\tau_s+\tau_b)$, and ω_b and ω_s refer to the bulk and surface NMR frequency. A fit to the higher-frequency branch of the data based on the frequency derivative of this equation gives the location of the peaks of the Fourier transform, or, equivalently, the frequency of the FID signals, and yields the curve shown in Fig. 7. The solid line of Fig. 5 shows the extension of this fit to the lower-frequency, i.e., surface, branch of the data. To obtain this fit, the wall shift was fixed at the measured value, and the binding energy was fixed at 1.04 K, leaving the sticking probability as the only free parameter. Since the temperature range over which data were taken varies by less than an order of magnitude, it is difficult to extract the temperature dependence of s. If we assume a linear dependence of s on temperature,[6–8] the best fit occurs for $s=[0.33(2)]T$. If we assume that s is a constant independent of temperature, the best fit occurs for $s=0.047$. Both lines are shown in the figure. Since the bulk data span only a factor of 3 in temperature, we cannot make an accurate determination of the temperature dependence of s.

The width of the higher-temperature bulk NMR line is

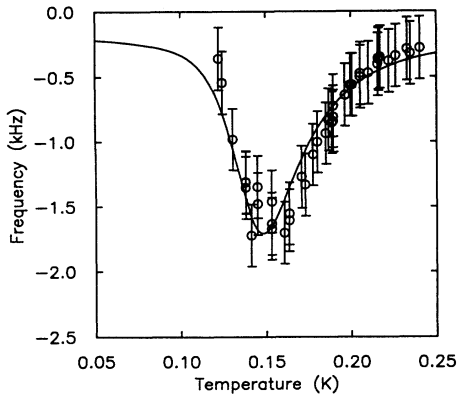

FIG. 7. A fit to the data points of the model of Eq. (11). As explained in the text, the wall shift and binding energy were fixed at their measured values; the only free parameter in the fit is the sticking coefficient. The solid line assumes that s has a linear dependence on temperature; the dashed line assumes that s is independent of temperature.

attributed to the inhomogeneity of the magnetic field across the sample, 0.6 G. As the temperature is decreased, the linewidth increases. We observe about a factor of 2 difference between a pure bulk trace ($T \approx 0.3$ K) and a lower-temperature trace ($T = 0.21$ K) when the line is broadened due to the finite residence time of the atoms on the surface. The linewidths of the bulk line at 0.21 K and of the surface line at 0.09 K are comparable. All of these measurements are consistent with the predictions of Eq. (11).

The surface signal that we measure corresponds to a surface density σ of about 10^{11} atoms/cm^2. The S/N ratio is determined by the low-temperature GaAs FET amplifier and allows detection of 9×10^{13} atoms at a bandwidth of 30 kHz. It was therefore necessary to signal average at least 1000 times to see a signal from the surface atoms. At the highest bulk densities ($n > 10^{16}$ atoms/cm^3), nuclear spin waves[3] were observed in our bulk signal.[28] For the wall-shift measurements we avoided frequency shifts from spin waves by operating in a regime in which the density is too low for spin-wave propagation. At the lower temperatures ($T < 200$ mK), it was necessary to run the discharge continuously due to an observed rapid loss of polarization which we believe is due to one-body processes (see below). However, by comparing the phase of the signal to that of a bulk signal of a known polarization, we believe that the surface gas is nuclear spin polarized.

The addition of small amounts of ^{3}He to the ^{4}He film significantly changes the characteristics of the surface presented to the hydrogen atoms. The binding energy to the surface is decreased by almost a factor of 3 (Ref. 12) due to the lower density of the ^{3}He atoms. This decrease in binding energy has a marked effect on the surface-bulk dynamics.[29] In addition, the thermal response time of the system increases, making temperature control difficult. Shifts of the bulk resonance frequency have been observed in this experiment, but are not reproducible. The largest shift that we observed appears to be about one-half of the size of the largest shift on the pure ^{4}He surface.

Uncertainty in the frequency plotted in Fig. 7 arises from the stability of the spectrometer. The width of the symbols used in Fig. 7 is consistent with the much smaller error bars associated with both the temperature calibration and temperature variations due to the instability of the discharge at low temperatures. The longer time constants that occur when ^{3}He is added, as well as our estimates of the relative thermal conductivities of the quartz and the ^{4}He film, lead us to believe that the superfluid is primarily responsible for heat transport from the film-covered plates to the copper cell.

From these experiments we find the wall shift measured on a substrate that is parallel to the magnetic field and extrapolated to zero field is $-43.2(10)$ kHz. The first direct measurement of the wall shift was made with NMR studies on a substrate that had no preferential orientation with respect to the magnetic field.[29] The measured wall shift extrapolated to zero field from that work is $-44.8(10)$ kHz. The only other measurements of the wall shift are from the work of Morrow *et al.*[30] in which it was extracted as a parameter in a fit to NMR data taken at temperatures at which the atoms spend only a small fraction ($\approx 10^{-3}$) of their time adsorbed on the surface. Their value is $\delta = -61$ kHz. The results of a second, similar experiment yielded $\delta = -71.5(30)$ kHz.[31] Our value for the sticking probability, $s = [0.33(2)]T$, is in excellent agreement with the results of both Berkhout *et al.*[8] and Helffrich *et al.*[9] It is pleasing to note the close agreement among these three measurements which were made with very different techniques.

B. Decay measurements

It would be of great interest to extend the above measurements to a lower-temperature regime where the surface gas can be studied with NMR. Interesting phenomena to examine in the two-dimensional gas in this regime include diffusion[1] and nuclear spin waves,[2] as well as the Kosterlitz-Thouless transition[4] at higher surface densities. We have made measurements of the decay of the atomic gas by monitoring the pressure transducer which indicate that there is a large one-body rate resulting in rapid depolarization and thermalization of the lower two states. The rapid loss of sample and subsequent heating due to recombination is the limiting factor in achieving higher surface densities. The origin of this process is unknown; an electron microscope scan of the surface does not reveal the presence of any magnetic impurities.

The focus of these experiments is the characterization of the decay of the atomic gas since future surface work depends on the ability to obtain good polarization. The second version of the cell which has been previously described was used because of its larger area to volume ratio and increased surface area. We preserved the geometry since the orientation of surface area with respect to the magnetic field is an important factor in analyzing the decay rates. A number of decay measurements were taken as a function of temperature and magnetic field by monitoring the signal from the pressure transducer. In addition, several different H_2 coatings

were explored to reduce the one-body rate. We found that it was possible to decrease the one-body rate by almost an order of magnitude by putting down a thick layer of molecular hydrogen (about 1000 Å assuming uniform coating of all surfaces inside of the NMR can). This reduction of the one-body relaxation rate allowed us to make a measurement of the two-body dipolar relaxation rate on the surface.

The time evolution of the density after the source is turned off is compared to a model based on Eq. (10) in a regime where the polarization is close to unity. It is necessary to fix $L_{\rm eff}$ to the existing experimental values[12] to obtain values for both the one- and two-body decay constants. The results for $G_{\rm eff}$ as a function of temperature are shown in Fig. 8 assuming the two possible temperature dependences of L_s: $L_s \propto \sqrt{T}$ or L_s independent of T. The line through the points is a fit to Eq. (5), fixing the two-body bulk rate to the value of Ref. 14. For the case of L_s independent of temperature, the best fit yields $G_s=[2.5(3)]\times10^{-14}$ cm^2/sec as shown in Fig. 8(a). The line in Fig. 8(b) corresponds to $G_s=[2.9(3)]\times10^{-14}$ cm^2/sec for $L_s \propto \sqrt{T}$. Figure 9 shows measured values of the magnetic field dependence of $G_{\rm eff}$ at a fixed temperature $T=0.236$ K. The solid curve is generated by fixing the relaxation rate to its measured value at $B=7.62$ T and calculating the expected field dependence. At these temperatures the relaxation is dominated by surface processes, thus the field dependence is calculated from Eq. (6).

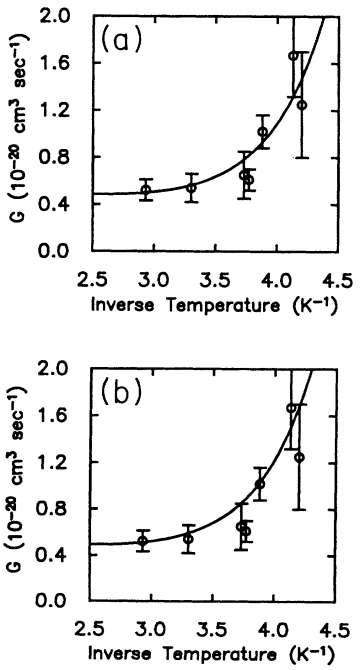

FIG. 8. Data from decay measurements at 7.62 T are fit to Eq. (5). G_b is fixed at the previously measured value of Ref. 12. In (a) the surface three-body rate has been fixed and is assumed to be independent of temperature. In (b) the surface three-body rate is assumed to have a square-root dependence on temperature. The best fit to the data as pictured occurs for $G_s=[2.5(3)]\times10^{-14}$ cm^2/sec for the case of (a), and $G_s=[2.9(3)]\times10^{-14}$ cm^2/sec for the case of (b).

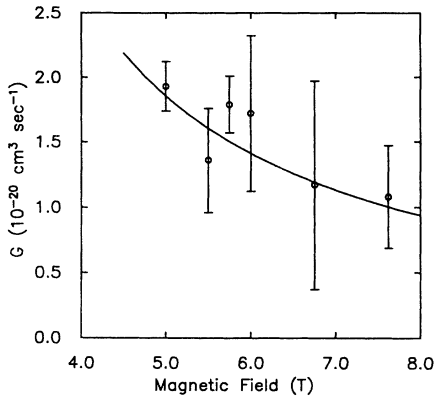

FIG. 9. The magnetic field dependence of $G_{\rm eff}$ is shown for a fixed value of $T=0.24$ K. The solid curve is generated by fixing the relaxation rate at its measured value at 7.62 T and calculating the expected field dependence. At these temperatures the relaxation is dominated by surface processes, as a result the field dependence is expected to be that of the surface rate.

The temperature dependence of the effective bulk one-body rate $R_{\rm eff}$ is shown in Fig. 10(a). The surface rate R_s can be extracted from

$$R_{\rm eff}=R_s\frac{A}{V}\Lambda\exp\left[\frac{E_b}{kT}\right]. \tag{12}$$

Figure 10(b) shows that the magnitude of R_s is about 10^{-2} sec^{-1} after coating with molecular hydrogen. In the first cell the average value of R_s was about 10^{-1} sec^{-1}. Thus, we have reduced the one-body rate by almost an order of magnitude by coating the surfaces below the ^{4}He film with molecular hydrogen. Another order of magnitude reduction in R_s is required to make the contribution to the recombination rates smaller than that from G_s in the relevant regime. The field dependence of $R_{\rm eff}$

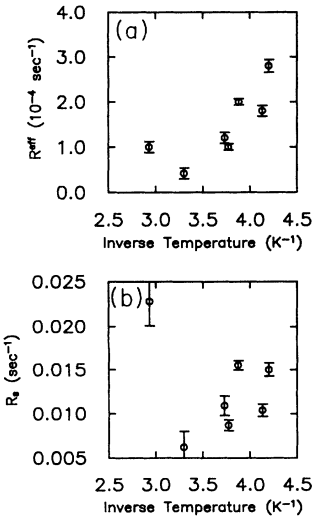

FIG. 10. (a) shows the measured value of the effective one-body bulk rate as a function of inverse temperature at $B=7.62$ T. (b) shows the surface rate extracted from the previous data according to Eq. (13).

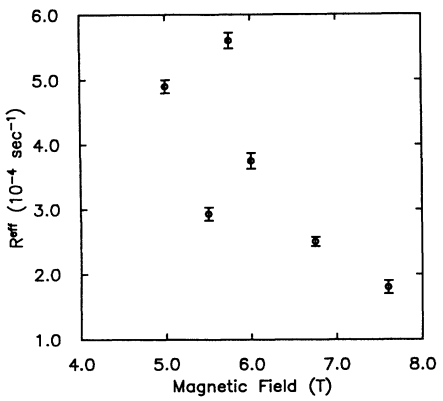

FIG. 11. The data represent measured values of the bulk one-body rate measured as a function of magnitude field at $T=0.24$ K.

was also measured at $T=0.236$ K and is shown in Fig. 11. The rate appears to increase with decreasing field in agreement with the predictions of Ref. 18. Since we have very few data points and there is a significant amount of scatter, it is difficult to draw detailed conclusions about the field dependence.

To summarize, we have measured the surface two-body relaxation rate, G_s, due to collisions between adsorbed H atoms in the temperature range 0.2–0.4 K. At higher temperatures the decay is dominated by the two-body bulk rate; at lower temperatures it is dominated by the three-body surface rate. We find for surfaces oriented parallel to the external field and assuming that L_s is independent of temperature, $G_s=[2.5(3)]\times10^{-14}$ cm^2/sec. The only other measurement of this rate, from observations of the decay of the gas using ESR techniques,[32] yields $G_s=4\times10^{-14}$ cm^2/sec. However, in that experiment, the orientation of the surfaces with respect to the magnetic field was not well defined. The theory of v.d. Eijnde *et al.*[17] predicts $G_{s,2}=2.0\times10^{-14}$ cm^2/sec ($G_{s,2}=G_s$ for our orientation) which is slightly smaller than our measured value. We have also measured the field dependence of G_s and find that it increases with decreasing field as predicted by the theory.

V. CONCLUSIONS

We have been able to obtain and measure surface densities of about 10^{11} atoms/cm^2 with NMR techniques. Higher surface densities will decay quickly due to the three-body rate. If the surfaces can be oriented at right angles to the magnetic field, the two-body surface rate is expected to vanish. Thus, if the one-body rate can be eliminated, a gas of this density will be stable for long periods of time.

In addition to the results already described, we have observed bulk spin waves in the gas at temperatures above 0.175 K. These modes have been extensively studied by the Cornell group.[3] An obvious extension of this work is the search for spin-wave modes among the atoms that are adsorbed to the surface.[2] Again, the one-body rate must be very small in order to preserve the polarization necessary to observe the spin-wave modes.

In conclusion, we feel that NMR is a very useful tool for the separate study of the bulk and surface populations in this system. We have been able to reduce the one-body rate by an order of magnitude, and have been able to measure several important parameters of the bulk-surface system. Future surface work, including the observation of surface spin waves or of the Kosterlitz-Thouless transition,[4] should be possible if another order of magnitude reduction can be achieved in the one-body rate.

ACKNOWLEDGMENTS

We would like to acknowledge D. Kleppner and Y. M. Xiao for discussions about the work, N. Erikson for the loan of the GaAs FET amplifier, and E. Smith for useful comments about the manuscript. This work was supported by the National Science Foundation under Grant No. DMR-8418718.

*Present address: Physics Department, Cornell University, Ithaca, NY 14853.

†Present address: Stanford University, Stanford, CA 94305.

[1]D. S. Zimmerman and A. J. Berlinsky, Can. J. Phys. **62**, 590 (1984).

[2]J. M. V. A. Koelman, H. H. M. F. Noteborn, L. P. H. de Goey, B. J. Verhaar, and J. T. M. Walraven, Phys. Rev. B **32**, 7195 (1985); E. P. Bashkin, Pis'ma Zh. Eksp. Teor. Fiz. **40**, 383 (1984) [JETP Lett. **40**, 1197 (1985)].

[3]B. R. Johnson, J. S. Denker, N. Bigelow, L. P. Levy, J. H. Freed, and D. M. Lee, Phys. Rev. Lett. **52**, 1508 (1984).

[4]D. O. Edwards and I. B. Mantz, J. Phys. (Paris) Colloq. **41**, C7-257 (1980).

[5]P. Zitzewitz and N. R. Ramsey, Phys. Rev. A **3**, 51 (1971).

[6]V. V. Goldman, Phys. Rev. Lett. **56**, 612 (1986).

[7]D. S. Zimmerman and A. J. Berlinsky, Can. J. Phys. **61**, 508 (1982).

[8]J. J. Berkhout, E. J. Wolters, R. van Roijen, and J. T. M. Walraven, Phys. Rev. Lett. **57**, 2387 (1986).

[9]J. A. Helffrich, M. P. Maley, and M. Krusius, Phys. Rev. B **1**, 2003 (1990).

[10]R. Jochemsen, M. Morrow, A. J. Berlinsky, and W. N. Hardy, Phys. Rev. Lett. **47**, 852 (1981).

[11]B. W. Statt and A. J. Berlinsky, Phys. Rev. Lett. **45**, 105 (1980).

[12]D. A. Bell, H. F. Hess, G. P. Kochanski, S. Buchman, L. Pollack, Y. M. Xiao, D. Kleppner, and T. J. Greytak, Phys. Rev. B **34**, 7670 (1986).

[13]T. J. Greytak and D. Kleppner, in *New Trends in Atomic Physics,* Proceedings of the Les Houches Summer School of Theoretical Physics, 1982, edited by G. Greenberg and R. Stora (North-Holland, Amsterdam, 1984), p. 1125.

[14]R. W. Cline, T. J. Greytak, and D. Kleppner, Phys. Rev. Lett. **47**, 1195 (1981).

[15]I. F. Silvera and J. T. M. Walraven, in *Progress in Low Temperature Physics, Volume X,* edited by D. F. Brewer (Elsevier Science, New York, 1986), p. 139.
[16]R. M. C. Ahn, J. P. H. W. v. d. Eijnde, and B. J. Verhaar, Phys. Rev. B **27**, 5424 (1983); B. W. Statt, *ibid.* **25**, 6035 (1982); A. Lagendijk, *ibid.* **25**, 2054 (1982); A. E. Ruckenstein and E. D. Siggia, *ibid.* **25**, 6031 (1982).
[17]J. P. H. W. v. d. Eijnde, C. J. Reuver, and B. J. Verhaar, Phys. Rev. B **28**, 6309 (1983).
[18]A. J. Berlinsky, W. N. Hardy, and B. W. Statt, Phys. Rev. B **35**, 4831 (1987).
[19]V. B. Kazanskii, G. B. Pariiskii, I. V. Aleksandrov, and G. M. Zhidomirov, Fiz. Tverd. Tela (Leningrad) **5**, 649 (1963) [Sov. Phys. Solid State **5**, 473 (1963)]; J. A. Weil, J. Chem. Phys. **71**, 2803 (1979).
[20]M. R. Morrow, Ph.D. thesis, University of British Columbia, 1983.
[21]W. N. Hardy, M. Morrow, R. Jochemsen, and A. J. Berlinsky, Physica B **109&110**, 1964 (1982).
[22]See references within Refs. 13 and 15.
[23]Acheson Colloids, Co., Port Huron, MI 48060.
[24]GC Electronics, Rockford, IL 61101.
[25]D. S. Greywall and P. A. Busch, J. Low Temp. Phys. **46**, 451 (1982).
[26]Phil Adams and Harald Hess (private communication).
[27]P. W. Anderson and P. R. Weiss, J. Phys. Soc. Jpn. **9**, 316 (1954).
[28]L. Pollack, Ph. D. thesis, Massachusetts Institute of Technology, 1989.
[29]L. Pollack, S. Buchman, Y. M. Xiao, H. F. Hess, G. P. Kochanski, and T. J. Greytak, Phys. Rev. B **34**, 461 (1986).
[30]M. Morrow, R. Jochemsen, A. J. Berlinsky, and W. N. Hardy, Phys. Lett. **46**, 195 (1981); **47**, 455(E) (1981).
[31]W. N. Hardy, M. D. Hurlimann, and R. W. Cline, Proceedings of the 18th International Conference on Low Temperature Physics [Jpn. J. Appl. Phys. **26**, 2065 (1987)].
[32]M. W. Reynolds, I. Shinkoda, W. N. Hardy, A. J. Berlinsky, F. Bridges, and B. W. Statt, Phys. Rev. B **31**, 7503 (1985).

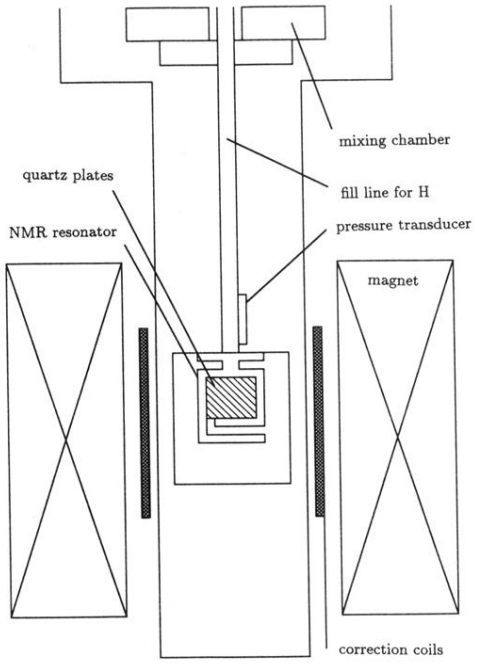

FIG. 3. A schematic of the apparatus is shown below the level of the mixing chamber of the dilution refrigerator.